

Ultra-low dose CT of the chest at 0.18 mSv: comparison of a novel projection technique with conventional chest x-ray

Poster No.: C-3543
Congress: ECR 2019
Type: Scientific Exhibit
Authors: S. Carey¹, S. Kandel¹, J. Kavanagh², T. Chung¹, C. Farrell¹, P. Rogalla¹; ¹Toronto, ON/CA, ²Toronto/CA
Keywords: Thorax, Lung, CT, Image manipulation / Reconstruction, Computer Applications-General, Radiation safety, Artifacts, Dosimetric comparison
DOI: 10.26044/ecr2019/C-3543

Any information contained in this pdf file is automatically generated from digital material submitted to EPOS by third parties in the form of scientific presentations. References to any names, marks, products, or services of third parties or hypertext links to third-party sites or information are provided solely as a convenience to you and do not in any way constitute or imply ECR's endorsement, sponsorship or recommendation of the third party, information, product or service. ECR is not responsible for the content of these pages and does not make any representations regarding the content or accuracy of material in this file.

As per copyright regulations, any unauthorised use of the material or parts thereof as well as commercial reproduction or multiple distribution by any traditional or electronically based reproduction/publication method is strictly prohibited.

You agree to defend, indemnify, and hold ECR harmless from and against any and all claims, damages, costs, and expenses, including attorneys' fees, arising from or related to your use of these pages.

Please note: Links to movies, ppt slideshows and any other multimedia files are not available in the pdf version of presentations.

www.myESR.org

Aims and objectives

Conventional chest x-ray (CXR) is often used as a first-step diagnostic tool as it is cheaper, quicker, and has a reduced radiation dose as compared to standard computed tomography (CT). Conversely, CXR suffers from reduced sensitivity and carries an increased false-negative rate for many indications[1][2][3][4]. The primary advantage then of CXR with respect to patient health is the reduced radiation exposure.

The effective radiation dose of an Ultra Low-Dose (ULD) CT protocol can be lowered to a similar range as that of plain film radiography (~0.18 mSv), however, increased voxel noise is incurred as a tradeoff with reduced dose. The increased noise can be mitigated by suitable post-processing; to this end we refine a projection algorithm introduced in a prior work[5] and apply it to ULDCT images to produce a new thick-slice image, henceforth the thoracic tomogram.

The aim of the study was to compare thoracic tomograms with CXR images with respect to clinical interpretation characteristics, time to read, and reader confidence.

Methods and materials

Projection Algorithm:

Similar to Maximum Intensity Projection (MIP), we create a thick-slab projection from thin-slice data by computing the Hounsfield Unit (HU) value at a given position (i, j, k) from the HU values of the voxels at positions $(i, j, k), (i, j, k+1) \dots (i, j, k+r)$, where r is the number of voxels satisfying: $l = r*w$, l is the desired output slice thickness and w is the width of one voxel in the thin-slice data. For MIP, the resultant CT number is the maximum CT number of the pertinent voxels. For our algorithm, we order the voxels by increasing CT number and apply a weight function to that ordered vector (Fig 1, 2), essentially creating a weighted average. Similar to a MIP function, the highest valued voxels receive the highest weight, producing an image with sharper contrast than by using an average projection. Unlike MIP, none of the CT number information is discarded, providing a higher resilience to voxel noise. For further details about the weight function, see[5]. An example of a thoracic tomogram is shown in Fig. 3.

Study Methodology:

To evaluate the thoracic tomogram we prepared a dataset of 22 cases of patients who had undergone a CXR and a same day standard-of-care non-contrast CT of the chest (with mean DLP 44.1). Scanner specific noise was added to the raw projection data to simulate the target dose of 0.18mSV. Coronal and sagittal isotropic images were reformatted from axial reconstructions with a slice thickness of 0.8mm. The projection algorithm was then applied to produce 2cm thick slabs with a 1cm overlap.

The x-rays and thoracic tomograms for the 22 cases were ordered randomly, producing a sequence of 44 images. These cases were then reviewed by three chest radiologists with no prior training for the study. They recorded, on a scale from -4 (definitely absent/normal) to +4 (definitely present/abnormal) their impression with respect to 13 diagnostic categories (Fig 4).

The ground truth, collected from the original CT reports, was compared to the reader's response for the x-ray and thoracic tomogram for each category. ROC curves were generated for each category. The time for interpretation and reader's image satisfaction score (from 1 to 10) were also recorded and statistically compared.

Images for this section:

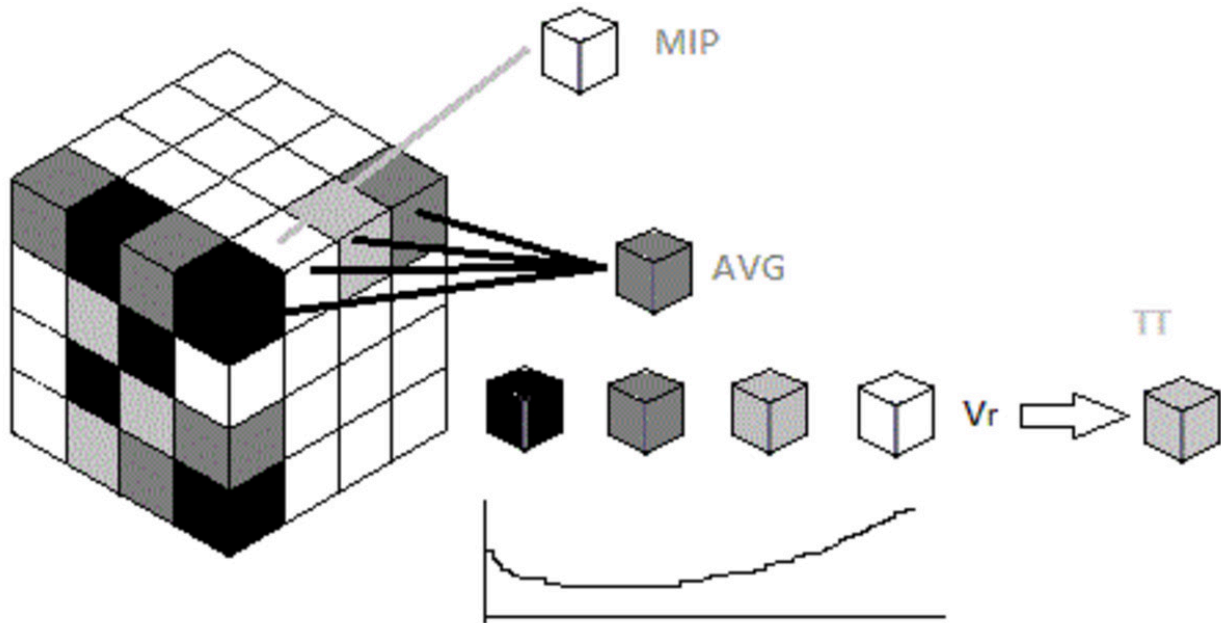


Fig. 1: Visualization of projection algorithm.

© Joint Department of Medical Imaging, University of Toronto - Toronto/CA

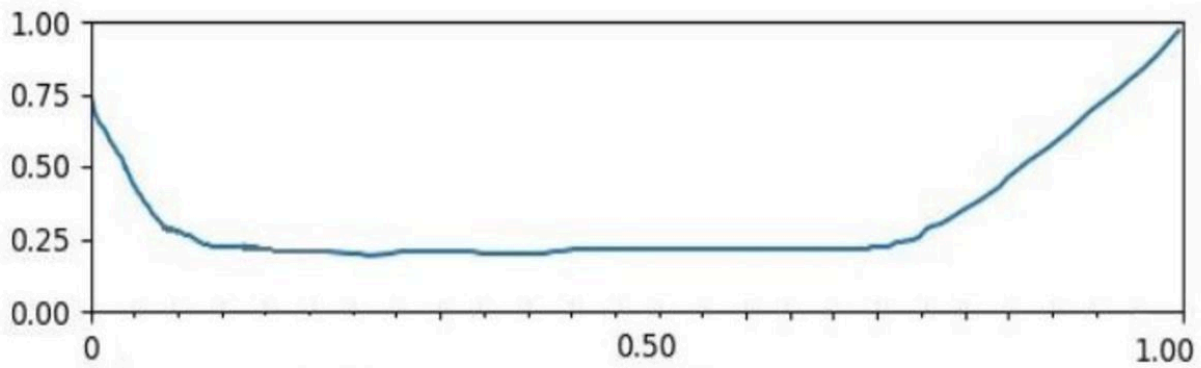


Fig. 2: Weight function used. X-axis is position in voxel vector, y-axis is weight amount.

© Joint Department of Medical Imaging, University of Toronto - Toronto/CA

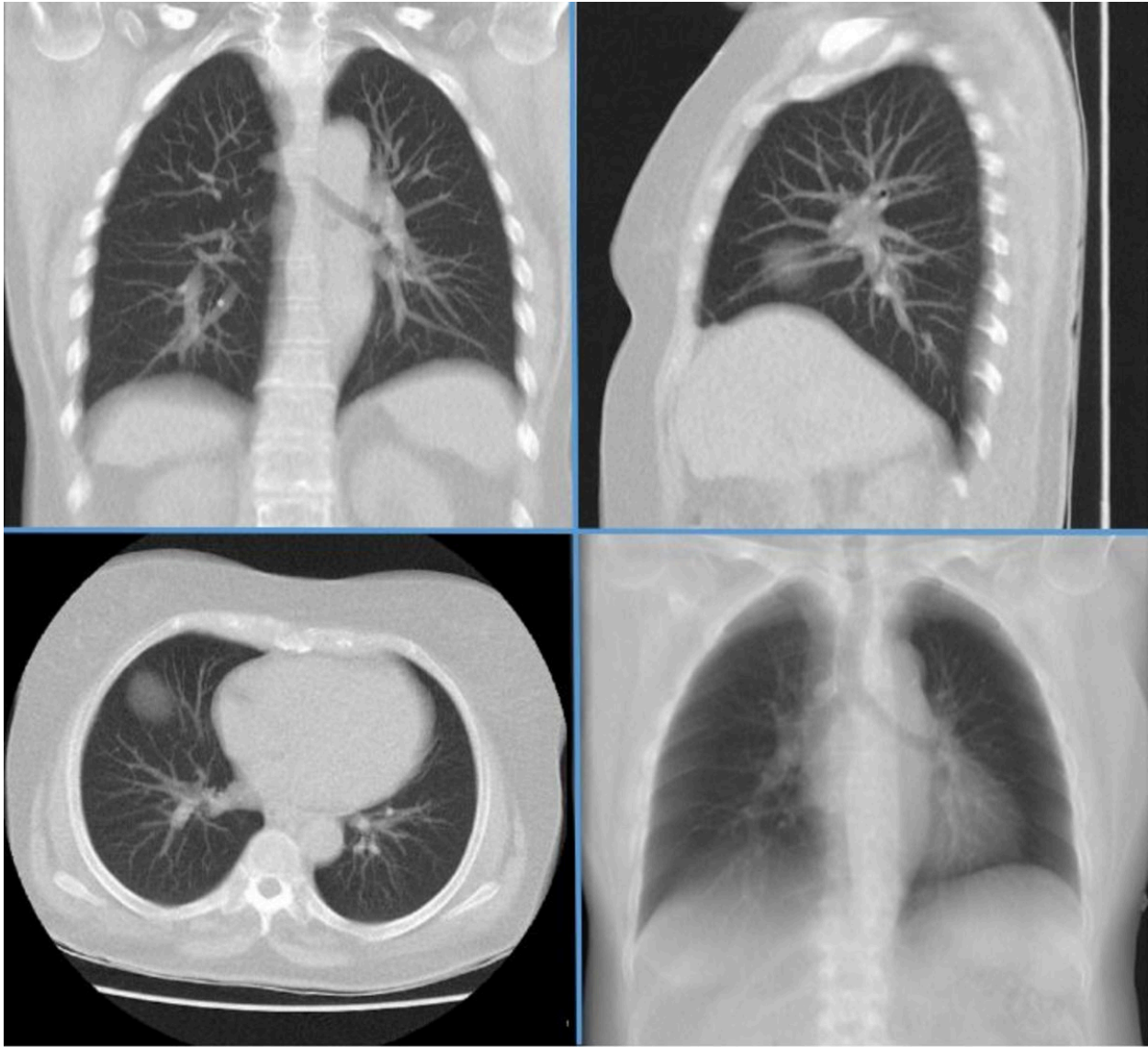


Fig. 3: Single 2cm slice from coronal, sagittal, and axial views of a thoracic tomogram. The final coronal view is a 10cm, x-ray-like single slice created by average projection.

© Joint Department of Medical Imaging, University of Toronto - Toronto/CA

Results

The area under the ROC curve was measured for each assessment category (Fig 4). The average area under the curve for each category increased by .276, or ~45%.

The mean time for interpretation and image quality score for X-rays/thoracic tomograms was 24.0s/36.9s ($p=0.07$), and 7.8/8.2 ($p=0.16$), respectively. To have a rough comparison of the noise in the three discussed projection techniques, a histogram was taken for a 70x70 region in the liver of an image which was processed with average projection, MIP, and thoracic tomogram projection (Fig 5). The standard deviation of this region for each image is measured to be: MIP: 4.581 HU, AVG: 2.520 HU, Thoracic Tomogram: 2.517 HU.

Images for this section:

	Pneumonia	Pulmonary Edema	Interstitial Lung Disease	Nodules $\geq 5\text{mm}$	Nodules $< 5\text{mm}$	Pleural Effusion	Pericardial Effusion	Heart Size	Mediastinal Vessels	Pneumothorax	Acute Bone Fractures	Foreign Bodies	Free Abdominal Air
X-Ray	0.61	0.11	0.33	0.65	0.53	0.72	0.86	0.43	0.41	0.98	0.51	0.80	1.0
TT	1.0	1.0	0.83	0.89	0.57	0.86	0.86	1.0	0.98	0.98	0.55	1.0	1.0

Fig. 4: Area under ROC curve for each diagnostic category, x-ray and thoracic tomogram.

© Joint Department of Medical Imaging, University of Toronto - Toronto/CA

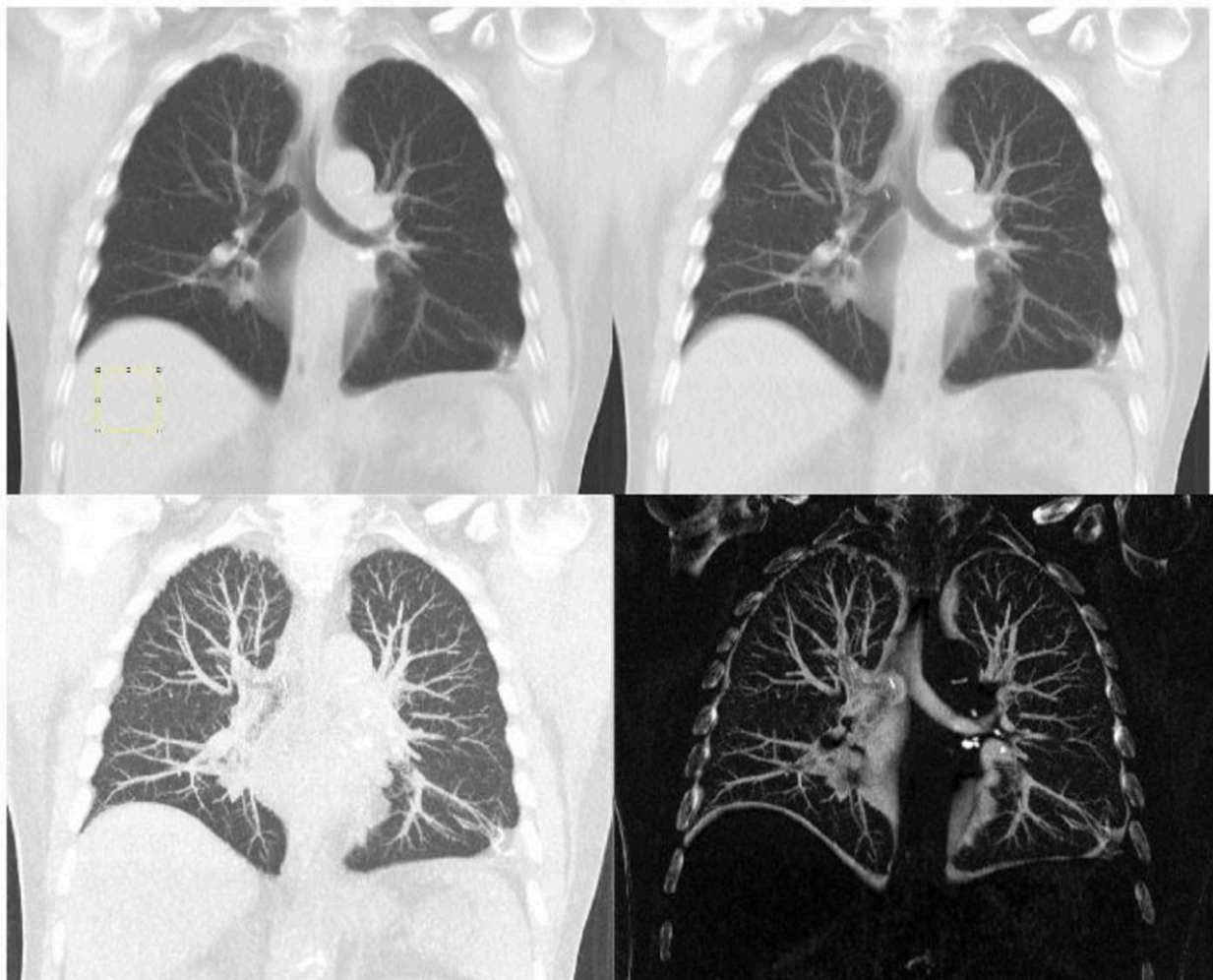


Fig. 5: Comparison of projection algorithms. From left to right: average, thoracic tomogram, MIP, average subtracted from thoracic tomogram. The subtractive image highlights the contrast gain of the thoracic tomogram projection over average projection.

Conclusion

The ROC area under the curve indicates a higher level of confidence almost across the board with a thoracic tomogram. This was expected as a multi-slice CT offers significantly more information than CXR, and in accordance the reading time is also increased by ~54%. In determining whether thoracic tomograms can be a suitable replacement for CXR, it will be prudent to assess how we value the tradeoff between confidence and interpretation time, as well as the importance of each diagnostic category.

Fig. 6 shows a comparison of a CXR and a single slice from a thoracic tomogram. A patient underwent a CXR and a same day standard-of-care non-contrast CT of the chest. This case was not used in the study, but instead is shown to demonstrate the significant diagnostic advantage of CT over CXR. In the thoracic tomogram a lung cancer is clearly demonstrated, while it is completely invisible in the CXR. This case is an example of how CXR can miss significant findings and emphasizes that CT offers more diagnostic information than CXR. We expect that the thoracic tomogram will offer greatly increased diagnostic sensitivity compared to CXR with a similar effective dose.

Images for this section:

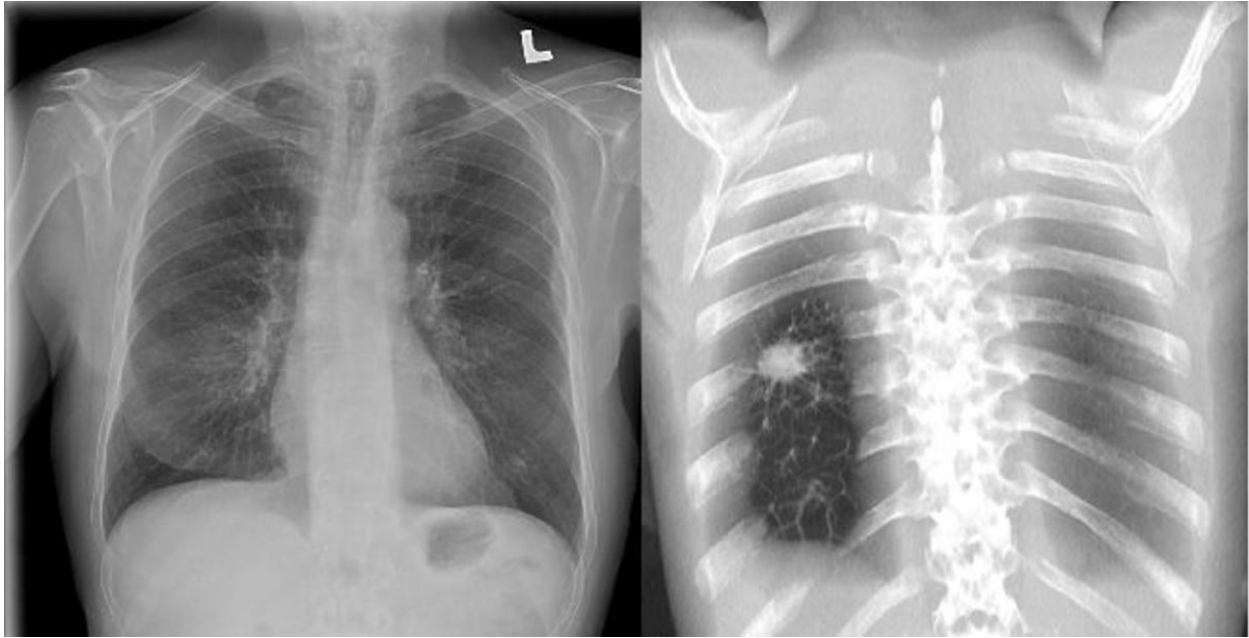


Fig. 6: CXR and single-slice thoracic tomogram comparison.

© Joint Department of Medical Imaging, University of Toronto - Toronto/CA

References

1. Maughan BC, Asselin N, Carey JL, Sucov A, Valente JH (2014) False-negative chest radiographs in emergency department diagnosis of pneumonia. *R I Med J.* 1;97(8):20-3.
2. van Beek EJ, Mirsadraee S, Murchison JT (2015). Lung cancer screening Computed tomography or chest radiographs? *World J Radiol.* 7(8):189-193.
3. Wesley H. Self, D. Mark Courtney, Candace D. McNaughton, Richard G. Wunderink, Jeffrey A. Kline (2014) High Discordance of Chest X-ray and CT for Detection of Pulmonary Opacities in ED Patients: Implications for Diagnosing Pneumonia. *Am J Emerg Med.* Feb; 31(2): 401-405.
4. Ziegler K, Feeny JM, Desai C, Sharpio D, Marshall WT, Twohig M (2013) Retrospective review of the use and costs of routine chest x rays in a trauma setting. *Journal of Trauma Management & Outcomes.*7:2-6.
5. Meyer H, Juran, R, Rogalla P (2008) softMip: A Novel Projection Algorithm for Ultra-Low-Dose Computed Tomography. *Journal of Computer Assisted Tomography.* 32(3): 480-484